A Study on the Condition Monitoring for GIS Using SVD in an Attractor of Chaos Theory

J.S. Kang*, C.H. Kim* and R.K. Aggarwal**

Abstract - Knowledge of partial discharge (PD) is important to accurately diagnose and predict the condition of insulation. The PD phenomenon is highly complex and seems to be random in its occurrence. This paper indicates the possible use of chaos theory for the recognition and distinction concerning PD signals. Chaos refers to a state where the predictive abilities of a systems future are lost and the system is rendered aperiodic. The analysis of PD using deterministic chaos comprises of the study of the basic system dynamics of the PD phenomenon. This involves the construction of the PD attractor in state space. The simulation results show that the variance of an orthogonal axis in an attractor of chaos theory increases according to the magnitude and the number of PDs. However, it is difficult to clearly identify the characteristics of the PDs. Thus, we calculated the magnitude on an orthogonal axis in an attractor using singular value decomposition (SVD) and principal component analysis (PCA) to extract the numerical characteristics. In this paper, we proposed the condition monitoring method for gas insulated switchgear (GIS) using SVD for efficient calculation of the variance. Thousands of simulations have proven the accuracy and effectiveness of the proposed algorithm.

Keywords: Chaos, Attractor Reconstruction, Partial Discharge, Singular Value Decomposition, Gas Insulated Switchgear

1. Introduction

In order to supply electric power with a high degree of reliability, the insulation diagnosis of high voltage power apparatus like SF6 gas insulated switchgear (GIS) is needed. Partial discharge (PD) measurement is a promising technique to prevent the breakdown in GIS and to maintain the high performance of electrical insulation. Substantial amounts of research related to the diagnosis technique for GIS has been reported [1], and various kinds of PD sensors, especially UHF sensors, have been developed. However, there exist external noises inside and outside GISs on-site. An advanced technique is indispensable to discriminate small PD signals in SF6 gas from large external noises and to improve the sensitivity for detecting harmful PD signals in GIS. Therefore, a PD identification technique needs to be developed [2].

PD is extremely complex and exhibits behavior that seems to be apparently random. It has been shown that the seemingly random behaviour of PD can be analysed by using chaos theory as a PD recognition tool [3].

In this paper, PD signals, which were denoised and normalized by wavelet transform, are transformed to surrogate data, and Takens embedding theory is used for attractor reconstruction of chaos theory following deciding time delay and embedding dimension. Although the orthogonal axis of the attractor increases according to the magnitude and the number of partial discharges, fault classification of GIS is complex. Therefore, singular value decomposition (SVD) and the principal component analysis (PCA) method are used to extract the numerical characteristics of the orthogonal axis of the attractor. The comparative results of the orthogonal axis of the attractor show that SVD is superior to PCA. Thus, we proposed the condition monitoring method for GIS using SVD using thousands of simulations to prove its accuracy and effectiveness.

* Dept. of Electrical and Computer Engineering, Sungkyunkwan University, Suwon-city, 440-746, Korea chkim@skku.edu).
** Dept. of Electronic and Electrical Engineering, University of Bath, Bath BA2 7AY, UK.
Received May 12, 2003 ; Accepted February 9, 2004

2. Chaos Theory

Fig. 1 shows the implementation process of chaos theory. In Fig. 1(a), measured signals are classified into 4 types; a constant signal after time passes, a periodic signal, a signal having two independent frequencies, and an irregular signal. To apply chaos theory to these signals, attractor reconstruction (a geometrical analysis method of the observed time series data) is necessary. Fig. 1(b) illustrates Takens embedding theory. After accurately determining time delay and embedding dimension, the time series data

can be diagrammed as attractor reconstruction. The attractor reconstruction of each time series is shown in Fig. 1(c). Respectively, the four signals from Fig. 1(a) contain characteristics of fixed point attractor, limit cycle attractor, torus attractor, and strange attractor. The dynamic characteristics of a measured signal can be geometrically defined by attractor reconstruction. Poincare surface, depicted in Fig. 1(d), is used in the case if the strange attractor. Poincare surface shows an attractor of complex structure to plane. Thus, we can interpret self-similarity, the Lyapunov exponent and the correlation dimension, just as in Fig. 1(e). Generally, the chaotic signal consists of fractal structure, with Lyapunov exponent larger than zero, and correlation dimension as a real number. Lyapunov exponent serves as proof of the chaotic nature of PD phenomenon, describes qualitatively dynamic behaviour of the attractor and is the average exponential rate at which the nearby trajectories diverge or converge.

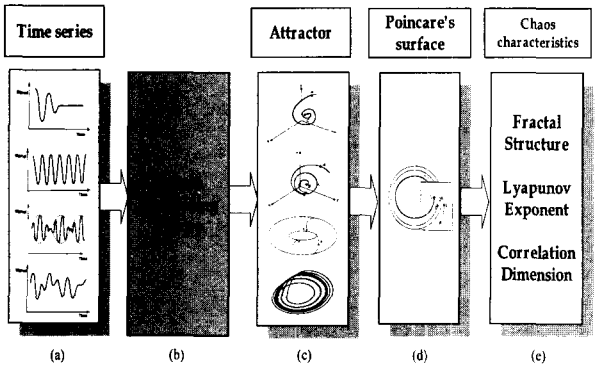

Fig. 1 Implementation process of Chaos Theory

3. Attractor of Chaos Theory

The concept of attractors is central in the idea of the use of chaos in PD recognition. In this paper, a defining attractor is broad enough to include all the natural candidates, but is restrictive enough to exclude the imposters. An attractor is a set to which all neighboring trajectories converge and a geometric form that characterizes long term behaviour in the state space, that is, it is what the behaviour of a dynamic system settles down to or is attracted to. Stable fixed points and stable limit cycles are examples [4].

3.1 Surrogate Data

Surrogate data is an ensemble of data sets similar to the raw data. A method used to do this is to take a Fourier transform of the raw data, randomize the phases, and then invert the Fourier transform. The resulting time series will have the same power spectrum as the raw data set, but will in all other respects be random. Significance has been proposed, which will allow for the detection of nonlinearity and can be expressed as follows:

$$Z = \frac{(r - \mu_{rs})}{\sigma_{TS}} \tag{1}$$

Where r is the nonlinear exponent value of time series, μ_{rs} is an average value for a nonlinear exponent value of the replacement data, and σ_{TS} is the standard deviation for the nonlinear exponent value of the replacement data [5].

3.2 Attractor Reconstruction

The attractor is a very important concept in the dynamical system. In chaotic systems, the attractor is usually referred to as a "strange attractor" due to its complicated shape. The strange attractor embodies all the dynamical properties of the system. Hence, if the attractor is quantified, the dynamical system can be characterized. There are two important parameters (embedding dimension and time delay) for display coordinate embedding and further application. Attractors that show the visual characteristics of PDs are classified as fixed point attractors, limit cycle attractors, torus attractors and strange attractors.

3.2.1 Time Delay and Embedding Dimension

Appropriate time delay and embedding dimension in the reconstruction process are important. If time delay is too small, $x(t)$ and $x(t+\tau)$ are excessively correlated and if time delay is too large, $x(t)$ and $x(t+\tau)$ are uncorrelated as completely random variables. Therefore, appropriate time delay is needed for phase space reconstruction. In other words, the appropriate time delay occurs when the coordinates $x(t)$ and $x(t+\tau)$ are independent but not completely uncorrelated so that they can be regarded as independent coordinates in the reconstructed phase space. The method to determine the appropriate time delay used is the correlation integral method suggested by Lidbert and Schuster. The correlation integral can be expressed as follows [6]:

$$C(r) = \frac{1}{N^2} \sum_{i=1}^{N} \sum_{j=1}^{N} \Theta(r - |X(i) - X(j)|) \tag{2}$$

Where Θ is step function, $X(i)$ and $X(j)$ are the points for ith and jth of the attractor, N is the number of data, r is a radius between two points, and $X(i) - X(j)$ is the Euclidean distance between two points. The method

of time delay can be used when the correlation integral becomes the first local minimum point.

To decide the embedding dimension, the False Nearest Neighbor method (FNN), suggested by Kennel, is used [7]. FNN is the method that decides the embedding dimension of the time series when the percentage of FNN gets near zero [%]. FNN percentage is calculated by dividing the FNN coefficient of each data by the total number of attractors.

3.2.2 Takens Embedding Theory

Attractor reconstruction of the time series uses the Takens embedding theory. If a time series is similar to $\xi_1,\xi_2,\cdots,\xi_i,\cdots$, this method is reconstructed to an orbit of attractor using the difference of the time delay. Definitely, m dimension vector in m dimension space, like in equation (3), is made from time series, ξ_t, and time delay, τ.

$$\begin{aligned} X_1 &= (\xi_1,\xi_{1+\tau},\xi_{1+(m-1)\tau}) \\ X_2 &= (\xi_2,\xi_{2+\tau},\xi_{2+(m-1)\tau}) \\ &\vdots \\ X_t &= (\xi_t,\xi_{t+\tau},\xi_{t+(m-1)\tau}) \\ &\vdots \\ X_N &= (\xi_N,\xi_{N+\tau},\xi_{N+(m-1)\tau}) \end{aligned} \tag{3}$$

Where τ is time delay and m is embedding dimension.

The time series, $\xi_1,\xi_2,\cdots,\xi_i,\cdots$, is expressed in one dimension. Applying the time delay and the embedding dimension is done using the method to express the phase plane concerning the signal of the measured system. Therefore, m dimension vector will cause each coordinate and phase plane trajectory to connect this point. Fig. 2 shows the attractor reconstruction in the phase plane applying the time delay, τ, and the embedding dimension, m.

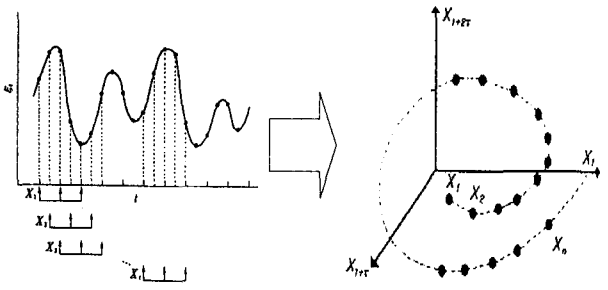

Fig. 2 Attractor reconstruction using Takens embedding theory

4. SVD and PCA

4.1 SVD (Singular Value Decomposition)

SVD of a rectangular matrix A is a decomposition of the form:

$$A = U\sum V^T \tag{4}$$

Where $U^TU = V^TV = I_n$ and $\sum = diag(\sigma_1,\cdots,\sigma_n),\sigma_i > 0$ for $1 \le i \le r,\sigma_j = 0$ for $j \ge r+1$. The first r columns of the orthogonal matrices U and V define the orthonormal eigenvectors associated with the r nonzero eigenvalues of AA^T and A^TA, respectively. The columns of U and V are referred to as the left and right singular vectors, respectively, and the singular values of A are the diagonal elements of the nonnegative square roots of the n eigenvalues of AA^T. As defined by the equation, the SVD is used to represent the original relationships among terms and documents as sets of linearly independent vectors or factor values. Using k factors or the k largest singular values and corresponding singular vectors, it is possible to encode the original term-by-document matrix as a smaller collection of vectors in k space for conceptual query processing.

4.2 PCA (Principal Component Analysis)

PCA is a technique widely used in the statistical community, primarily for descriptive but also for inferential purposes. It is often used to create a projection of multivariate data onto a space of lower dimensionality while attempting to preserve as much of the structural nature of the data as possible.

Let $W = (w_1,\cdots,w_N)$ be a N dimensional weight vector containing all the weights in a network $W \in R^N$. The weights are collected sequentially into this vector, from an input unit to each hidden unit in turn and from a hidden unit to each output (assuming there is a bias unit after the last normal node in the input and hidden layers). The training process produces a trajectory (data set) of points $W^j, j = 1\ldots s$ in weight space, on which PCA can be performed. This can be achieved by calculating the $N \times N$ covariance matrix Σ of this trajectory.

$$\Sigma = \frac{1}{s}\sum_{j=1}^{s}(W^S - \overline{W})(W^S - \overline{W})^T \tag{5}$$

Where $\overline{W}$ is the mean $\overline{W} = 1/s\sum_{j=1}^{s} W^j$.

The eigensystem of Σ is then found, providing a new set of basis vectors and a coordinate system. To reduce the dimensionality of the weight space to the value $d < N$, the d largest eigenvalues and corresponding eigenvectors are chosen and the remaining $N - d$ values are discarded. Performing this dimensionality reduction results in the smallest possible loss of variance information, for any other similarly defined choice of basis vectors. The direction of greatest variance in the data is given by the first principal component (eigenvector) V_i, corresponding to the largest principal value (eigenvalue) λ_i.

5. The Condition Monitoring Method for GIS

5.1 Time Series Analysis using Chaos Theory

5.1.1 Generation of Surrogate Data

Fig. 3 shows a denoised and normalized signal using wavelet transform of a PD signal. If an attractor reconstruction using this signal is made, it is complicated to extract the characteristics of the PD. This signal is difficult to reconstruct as an attractor because it has no inner structure. Fig. 4 shows the surrogate data made through phase randomization, which have linear characteristics and are useful to reconstruct as an attractor.

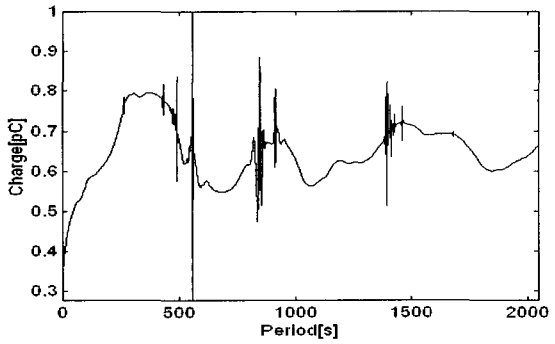

Fig. 3 Denoised and normalized signal

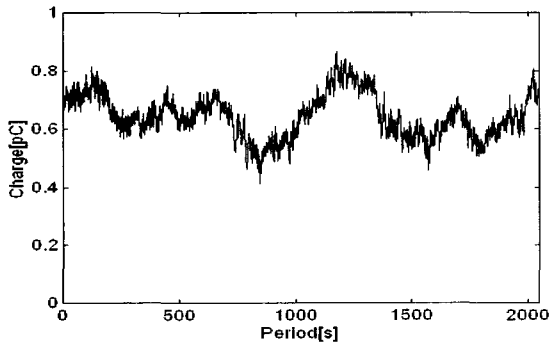

Fig. 4 Surrogate data

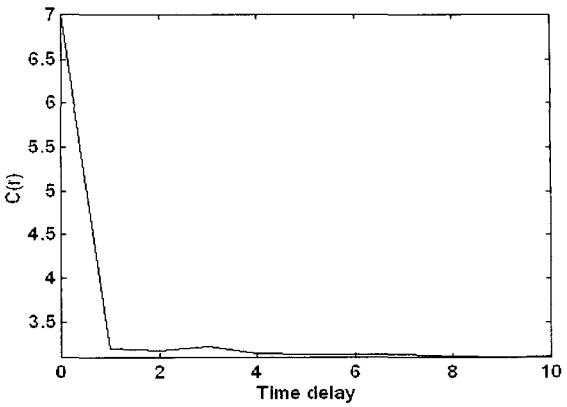

Fig. 5 Time delay

5.1.2 Decision of Time Delay and Embedding Dimension

Fig. 5 shows the simulation result for deciding time delay. We determined that time delay is 1 owing to the use of the correlation integral. Also, the embedding dimension is 2 to extract the characteristics of an attractor. Although it is difficult to extract characteristics greater than three dimensions, it is useful because of the function of Poincare surface.

5.1.3 Attractor Reconstruction

When we express PD in a phase plane, an attractor reconstruction of Takens embedding theory substituting time delay and embedding dimension is made. The simulation results indicated that the variance of an orthogonal axis in an attractor increases according to the magnitude and the number of partial discharges. Fig.s 6 to 9 show PD attractors, respectively, reconstructed 2-dimensionally using Takens embedding theory, with a time delay of 1, and an embedding dimension of 2. It can be seen, from the shapes in Fig.s 6 to 9, that the attractors are of straight line type. Hence, Fig.s 6 to 9 are normal GIS. In this case, the shape of an attractor with normal GIS is closed, has a central axis of 45°, and a very low orthogonal axis.

Fig. 10 shows attractor reconstruction in which PD is large and has three occurrences. Fig.s 11, 12, and 13 depict attractor reconstruction in which PD is large. Furthermore, Fig. 13 shows attractor reconstruction in which PD has eleven occurrences. When comparing these with attractors of normal GIS, we can see that the orthogonal axis of the attractors is increasing.

In addition, Fig.s 14 through 17 show simulation results with extreme PD. In attractor reconstruction, the orthogonal axis greatly changed and these Fig.s show that the orthogonal axis increased more than in the former simulation results. The shapes of the attractor are either line type or globe type.

When an attractor was reconstructed, we realized that

the orthogonal axis increased according to the magnitude and the number of PDs. Therefore, calculation of the orthogonal axis of an attractor in chaos theory and fault classification, using the calculated value, is possible. The occurrence of PD was discerned.

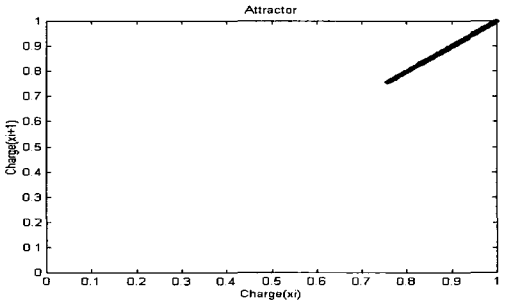

Fig. 6 Attractor reconstruction using measured signal of 6232A DS at WA GIS

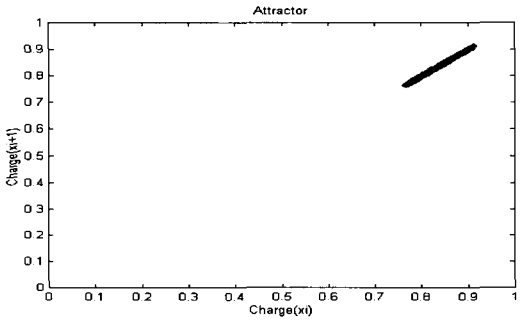

Fig. 7 Attractor reconstruction using measured signal of 611DS at SCP GIS

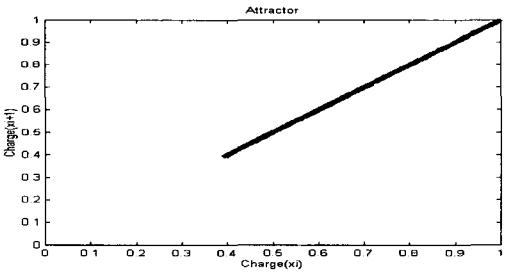

Fig. 8 Attractor reconstruction using measured signal of 622DS at CY GIS

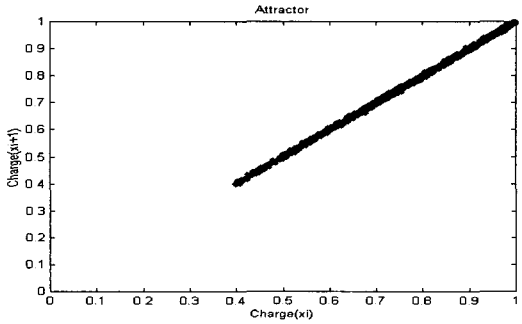

Fig. 9 Attractor reconstruction using measured signal of 697CB at GY GIS

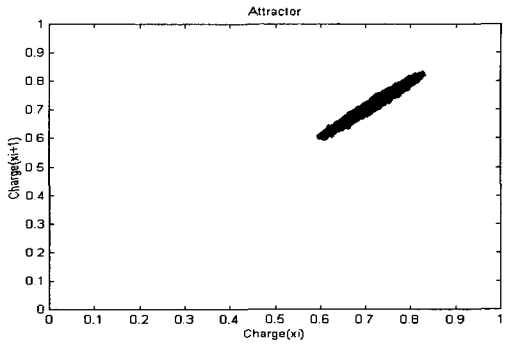

Fig. 10 Attractor reconstruction using measured signal of 611BDS at WA GIS

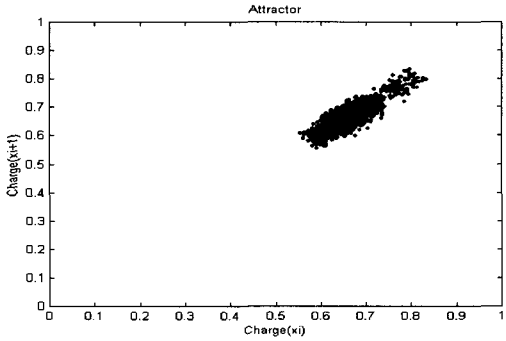

Fig. 11 Attractor reconstruction using measured signal of 6301DS at SW GIS

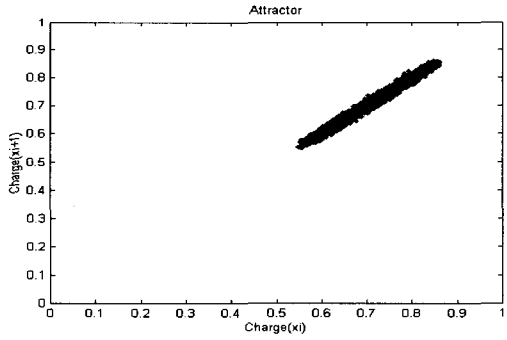

Fig. 12 Attractor reconstruction using measured signal of 616BDS at HD GIS

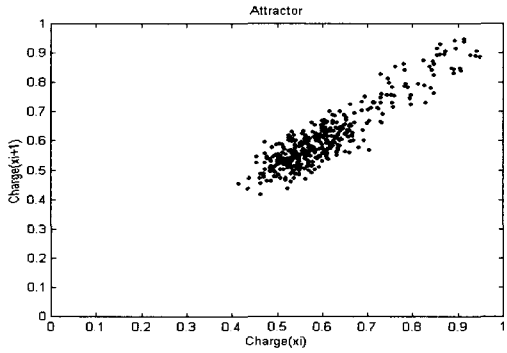

Fig. 13 Attractor reconstruction using measured signal of 616DS at JD GIS

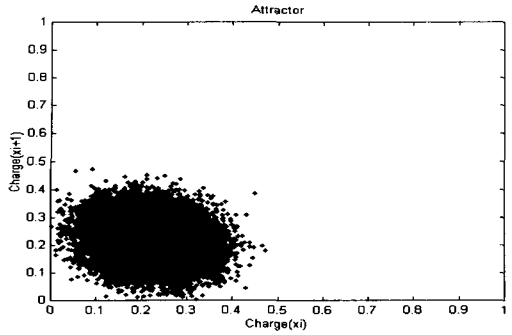

Fig. 14 Attractor reconstruction using measured signal of 6100CB at SCS GIS

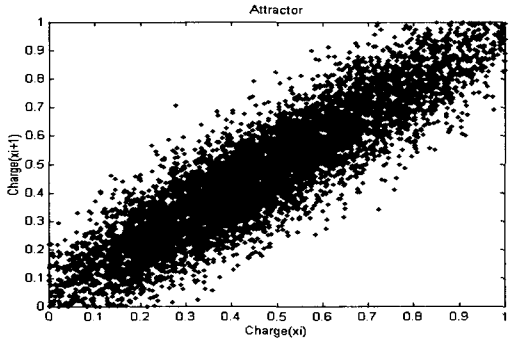

Fig. 15 Attractor reconstruction using measured signal of 682DS at WA GIS

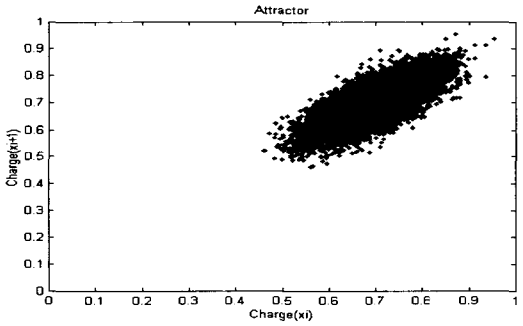

Fig. 16 Attractor reconstruction using measured signal of #1BUS at WY GIS

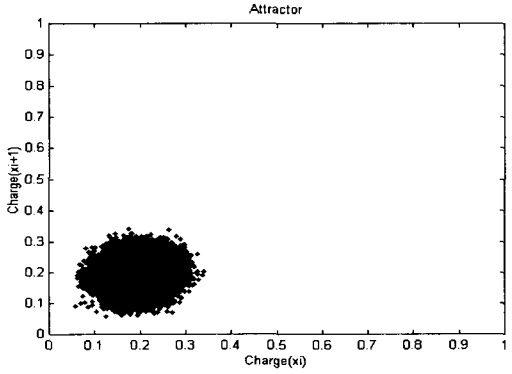

Fig. 17 Attractor reconstruction using measured signal of 6100CB at WY GIS

5.2 The Condition Monitoring Method for GIS using SVD

Fig. 18 shows the condition monitoring method for GIS using SVD suggested in this paper. The measured signal is denoised and normalized owing to external noise. Then, this denoised and normalized signal is transformed to surrogate data for attractor reconstruction. After deciding time delay and embedding dimension, the attractor is reconstructed by Takens embedding theory. The orthogonal axis of an attractor increases according to the magnitude and the number of PDs. At attractor reconstruction from Fig. 6 through 17, the secondary singular value of the variance of the orthogonal axis using SVD is shown in Table 1. Furthermore, Fig. 19 depicts correlation between the PD number and the secondary value. The region of the secondary singular value is determined and demonstrated in Fig. 18. If the secondary singular value is smaller than or equal to 0.4, GIS is in normal state and should be continuously observed. If the secondary singular value is larger than 0.4, it should be estimated that the secondary value is smaller than or equal to 0.7. If the secondary singular value is smaller than or equal to 0.7, a buzzer sounds and if the secondary singular value is larger than 0.7, the operator is flagged. Thus, it is useful to fault classification through variance calculations of the orthogonal axis using SVD. This algorithm demonstrated high reliability because the results of calculations using SVD are superior to those using PCA and this has been proven through thousands of simulations.

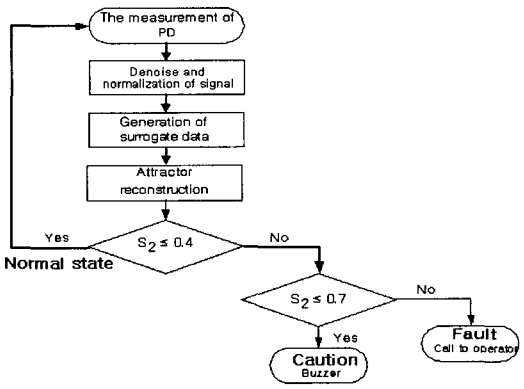

Fig. 18 Flow chart of condition monitoring method for GIS using SVD

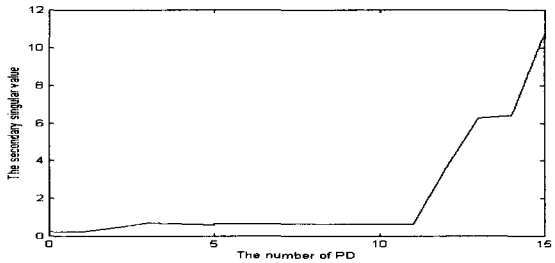

Fig. 19 Correlation of PD number and secondary singular value

Table 1 The Secondary Singular Value By SVD

Area	Position	The number of actual PDs	The secondary singular value
WA	6232ADS	0	0.1057
SCP	611DS	0	0.2584
CY	622DS	0	0.0928
GY	697CB	1	0.2398
WA	611BDS	3	0.6998
SW	6301DS	5	0.6751
HD	616BDS	5	0.5939
JD	616DS	11	0.6191
SGS	6100CB	Many	10.7792
WA	682DS	Many	6.2647
WY	#1BUS	Many	3.5514
WY	6100CB	Many	6.3992

Table 2 The Eigenvalue By PCA

Area	Position	The number of actual PDs	eigenvalue
WA	6232ADS	0	0.0000
SCP	611DS	0	0.0000
CY	622DS	0	0.0000
GY	697CB	1	0.0000
WA	611BDS	3	0.0000
SW	6301DS	5	0.0005
HD	616BDS	5	0.0001
JD	616DS	11	0.0100
SGS	6100CB	Many	0.0044
WA	682DS	Many	0.0019
WY	#1BUS	Many	0.0013
WY	6100CB	Many	0.0012

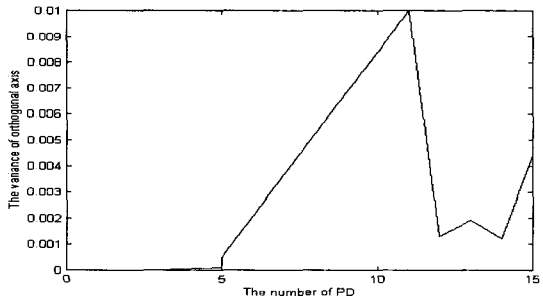

Fig. 20 Correlation of PD number and eigenvalue by PCA

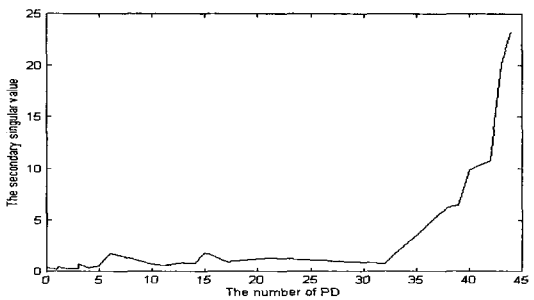

Fig. 21 Correlation of PD number and the secondary value

5.2 The Condition Monitoring Method for GIS using PCA

The calculated results concerning variance of orthogonal axis in an attractor using PCA are shown in Table 2. Furthermore, Fig. 20 presents the correlation of PD number and eigenvalue. Also, the flow chart of the condition monitoring method for GIS using PCA is the same as displayed in Fig. 18 except that $S_2 \leq 0.4$ is replaced with λ using PCA, and $S_2 \leq 0.7$ is omitted. It is difficult to grasp the PD occurrence because the eigenvalue of the PD is small and random according to the number and the magnitude of PDs.

Table 3 The secondary singular value region for fault classification

Region of the secondary singular value	State
$0<S_2 \leq 0.4$	Normal
$0.4<S_2 \leq 0.7$	Caution
$0.7<S_2$	Fault

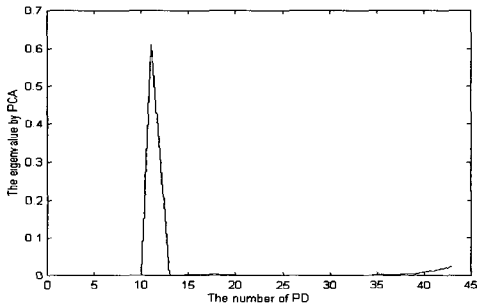

Fig. 22 Correlation of PD number and eigenvalue

6. Simulation Results and Discussion

6.1 Fault Classification for GIS using SVD

Simulation results using SVD, as shown in Table 4, indicate that the secondary singular value of normal GIS, where PD doesn't occur, is small, and that the secondary singular values of fault GIS is large in that the magnitude and the number of PDs are extreme. As the number of PDs increase, the secondary singular value also increases and Fig. 21 shows the correlation of the secondary singular value and the number of PDs. A few PDs can have large secondary singular values because the secondary singular value contains information regarding the number and the magnitude of the PD. Table 3 shows the region of the secondary singular value for fault classification.

Table 4 Simulation results Using SVD

State	Area	Position	The number of actual PDs	The Secondary singular value
Normal	MC	6231DS	0	0.1938
	WA	6232ADS	0	0.1057
	WA	6232CDS	0	0.3865
	HD	617CB	0	0.2225
	SCP	611DS	0	0.2584
	SC	6100CB	0	0.2726
	CY	#2BUS	0	0.2149
	CY	622DS	0	0.0928
	CY	622BDS	0	0.1281
	CY	622ADS	0	0.0942
	WL	617CB	0	0.2422
Caution	HD	616ADS	1	0.4163
Normal	GY	697CB	1	0.2398
	WA	6232BDS	1	0.3702
	WA	611DS	1	0.2490
	MC	6331DS	2	0.2655
Caution	WA	611B	3	0.6998
Normal	GS	622DS	3	0.3016
	GS	626DS	4	0.3477
Caution	SW	6301DS	5	0.6751
	HD	616BDS	5	0.5939
Normal	WL	612DS	6	1.7611
Fault	SCP	6233CB	10	0.7015
	WA	642DS	10	0.7521
Caution	JD	616DS	11	0.6191
Fault	SCP	6100CB	13	0.8697
	CD	647CB	13	0.8374
	GS	6100BUS	14	0.8374
	HD	616CDS	15	1.8397
	JD	626DS	17	0.9172
	YL	637DS	21	1.3320
	SC	622DS	32	0.8216
	HD	611DS	Many	23.2827
	SGS	644CB	Many	9.8516
Fault	SGS	641DS	Many	5.5044
	SGS	6100CB	Many	10.7792
	SGS	6101DS	Many	1.8323
	SC	6232DS	Many	20.1385
	GC	LsenceAll	Many	10.3578
	WA	682DS	Many	6.2647
	SW	6131DS	Many	4.4739
	JD	611DS	Many	2.6521
	WY	#1BUS	Many	3.5514
	WY	6100CB	Many	6.3992

Table 5 Simulation results using PCA

Area	Position	The number of actual PDs	eigenvalue
MC	6231DS	0	0.0000
WA	6232ADS	0	0.0000
WA	6232CDS	0	0.0001
HD	617CB	0	0.0000
SCP	611DS	0	0.0000
SC	6100CB	0	0.0000
CY	#2BUS	0	0.0000
CY	622DS	0	0.0000
CY	622BDS	0	0.0000
CY	622ADS	0	0.0000
WL	617CB	0	0.0000
HD	616ADS	1	0.0000
GY	697CB	1	0.0000
WA	6232BDS	1	0.0004
WA	611DS	1	0.0000
MC	6331DS	2	0.0000
WA	611B	3	0.0000
GS	622DS	3	0.0000
GS	626DS	4	0.0000
SW	6301DS	5	0.0005
HD	616BDS	5	0.0001
WL	612DS	6	0.0001
SCP	6233CB	10	0.0001
WA	642DS	10	0.0000
JD	616DS	11	0.6100
SCP	6100CB	13	0.0004
CD	647CB	13	0.0000
GS	6100BUS	14	0.0001
HD	616CDS	15	0.0014
JD	626DS	17	0.0032
YL	637DS	21	0.0001
SC	622DS	32	0.0000
HD	611DS	Many	0.0206
SGS	644CB	Many	0.0239
SGS	641DS	Many	0.0102
SGS	6100CB	Many	0.0044
SGS	6101DS	Many	0.0042
SC	6232DS	Many	0.0126
GC	LsenceAll	Many	0.0004
WA	682DS	Many	0.0019
SW	6131DS	Many	0.0001
JD	611DS	Many	0.0102
WY	1#BUS	Many	0.0013
WY	6100CB	Many	0.0012

6.2 Fault Classification for GIS using PCA

Table 5 shows the simulation results using PCA. As the number of PDs increase, the eigenvalue doesn't increase and Fig. 22 shows the correlation of the eigenvalues and the number of PDs. The eigenvalue of normal GIS is 0.0000 and the eigenvalue of fault GIS is also small. Hence, it is impossible to decide fault or normal state because the eigenvalue isn't constant.

In the simulation results, the calculation of the orthogonal axis in an attractor showed that SVD is superior to PCA and the proper establishment of the region of the secondary singular value using SVD is important for validity.

7. Conclusion

Detection of PD as the condition monitoring method for GIS is useful and many research outcomes concerning it are being reported. In this paper, we proposed the condition monitoring method for GIS using SVD in an attractor of chaos theory that was actively applied to the engineering field. Surrogate data has been compiled for attractor reconstruction of PD data. Once it was established that time delay is 1 and embedding dimension is 2, we could confirm that the variance of orthogonal axis increases in attractor reconstruction, as per Takens embedding theory. Simulation results using SVD and PCA indicated that SVD is superior to PCA. We proposed a reliable algorithm through simulation of numerous actual data as properly established regions of the secondary singular value.

Acknowledgements

The authors would like to acknowledge the financial and other support for this project provided by the Korea Science and Engineering Foundation(KOSEF). Project Number: 2000-2-30200-003-3

References

[1] Sakakibara T., Murase H., Haginomori E., Wakabayashi S., Emoto K., Ogawa A., "Study of propagation phenomena of partial discharge pulses in gas insulated substation", *IEEE Trans. on Power Delivery*, Vol. 13, No. 3, pp. 768-776, July 1998.

[2] Hoshino T., Kato K., Hayakawa N., Okubo H., "A novel technique for detecting electromagnetic wave caused by partial discharge in GIS", *IEEE Trans. on Power Delivery*, Vol. 16, No. 4, pp. 545-550, October 2001.

[3] Paithankar A.A., Mokashi A.D., "Recognition of PD faults using chaos mathematics", *Proceedings of the 1998 IEEE 6th International Conference on Conduction and Breakdown in Solid Dielectrics*, pp. 22-25, June 1998.

[4] Steven H.Stogatz, "*Nonlinear dynamics and chaos*", Addison-Wesley publishing company, 1994.

[5] J.H. Kim, J. Stringer, "*Applied chaos*", Electric Power Research Institute Palo Alto, 1992.

[6] J.D. Fraser, H.L. Swinney, "Independent coordinates for strange attractors from mutual information", *Physical Review A*, Vol. 33, pp. 1134, 1986.

[7] M.B. Kennel, "Determining Embedding Dimension for phase space reconstruction using geometrical construction", *Physical Reviews A*, Vol. 45, pp. 2403-3411. 1992.

Jin-Su Kang
He received his B.S. in Control and Instrumentation Engineering from Chungju University, Korea, 2001. He is now taking M.S. courses at Sungkyunkwan University. His main research interest is in the area of condition monitoring for GIS using chaos.

Chul-Hwan Kim (MIEEE)
He received his B.S. and M.S. degrees in Electrical Engineering from Sung kyunkwan University, Korea, 1982 and 1984, respectively. He received a Ph.D. in Electrical Engineering from Sungkyunkwan University in 1990. In 1990 he joined Cheju National University, Cheju, Korea, as a Full-time Lecturer. He was a Visiting Academic at the University of BATH, UK, in 1996, 1998 and 1999. Since March 1992, he has been a Professor in the School of Electrical and Computer Engineering, Sungkyunkwan University, Korea. His research interests include power system protection, artificial intelligence application to protection and control, the modeling/ protection of underground cable and EMTP software.

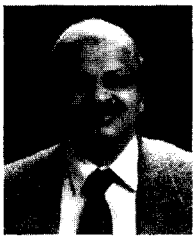

Raj Aggarwal (SMIEEE)
He obtained the degrees of B.Eng. and Ph.D. in Electrical Engineering from the University of Liverpool, UK, in 1970 and 1973, respectively. He then joined the Power and Energy Systems Group at the University of Bath, where he is now a Professor and Head of the Power and Energy Systems Group. His main research interests include power system modeling and the application of digital techniques and artificial intelligence to protection and control and power quality issues. He has published over 300 technical papers and is a fellow of the IEE UK.